Atmospheric Turbidity Forecasting using Side-by-side ANFIS

Julien Nou, Rémi Chauvin, Adama Traoré, Stéphane Thil, Stéphane Grieu

Available online at www.sciencedirect.com

SciVerse ScienceDirect

Energy Procedia 00 (2013) 000–000

Energy Procedia

www.elsevier.com/locate/procedia

SolarPACES 2013

Atmospheric Turbidity Forecasting Using Side-by-side ANFIS

J. Nou[1,*], R. Chauvin[1], A. Traoré[1,2], S. Thil[1,2], S. Grieu[1,2]

[1]*PROMES-CNRS, Rambla de la thermodynamique, Tecnosud, 66100 Perpignan, France*
[2]*University of Perpignan Via Domitia, 52 Avenue Paul Alduy; 66860 Perpignan, France*

Abstract

In a context of sustainable development, enthusiasm for CSP technologies is developing. To achieve a better competitiveness of the CSP plants, the CSPIMP (Concentrated Solar Power efficiency IMProvement) project has been recently initiated. The main target is to develop a new procedure to improve steam turbine start up cycles, maintenance activities and advanced plant control schemes. One challenge of the project is to better forecast the solar resource in order to better manage the CSP plant. An important parameter to estimate or predict the solar radiation is the atmospheric turbidity. Indeed, the direct normal irradiance (DNI) under clear sky can be expressed as a function of extraterrestrial irradiation, a coefficient depending on the altitude of the site and on the atmospheric turbidity. This paper focuses then on forecasting this atmospheric turbidity at different time horizons (until 3 hours). The proposed forecast method consists of an adaptive network-based fuzzy inference system based on data selected from the NREL laboratory by using discrete wavelet transform. From the ANFIS model developed and its different blocs, future values of atmospheric turbidity are then obtained. The best configuration for the tools used leads to satisfactory forecasting results and validates the proposed ANFIS methodology.

Selection and peer review by the scientific conference committee of SolarPACES 2013 under responsibility of PSE AG.

Keywords: Atmospheric turbidity; adaptive network-based fuzzy inference system; principal component analysis; wavelet-based multi-resolution analysis.

1. Introduction

Accurate knowledge of direct normal irradiance (DNI) under clear sky conditions is of high interest in many solar energy applications like concentrated solar power (CSP).

* Corresponding author. Tel.: +33-468-68-2706; fax: +33-468-68-2213.
E-mail address: julien.nou@promes.cnrs.fr

Selection and peer review by the scientific conference committee of SolarPACES 2013 under responsibility of PSE AG.

Nomenclature

AG	asymmetric Gaussian
AM	altitude corrected air mass
A_s	altitude of the studied site
ANFIS	adaptive network-based fuzzy inference system
b	multiplicative coefficient depending on the altitude of the site
DBT	dry bulb temperature
FIT	similarity criterion
I_{bn}	direct normal irradiance
I_0	irradiance of the extraterrestrial solar radiation
PCA	principal component analysis
MAE	mean absolute error
MRE	mean relative error
SG	symmetric Gaussian
T_{LIP}	atmospheric turbidity from Ineichen and Perez

The present paper, as part of the CSPIMP (Concentrated Solar Power efficiency IMProvement) project, focuses on the development of a forecasting model of the atmospheric turbidity.

The CSPIMP project began in may 2012 and includes the PROMES-CNRS laboratory and three partners: ACCIONA Energía (world leader in the renewable sector), Thermodyn (specialized in the supply of turbomachinery and services for the Oil and Gas industry, from production to transportation and processing, as well as for the production of electricity in co-generation plants) and Nuovo Pignone (offers a large portfolio of highly reliable machinery and equipment for all segments of the oil & gas industry). The CSPIMP project focuses on optimizing the performance of CSP plants. Its main target is to develop a new procedure to improve steam turbine start up cycles, maintenance activities and advanced plant control schemes. One challenge of the project is to better forecast the solar resource in order to better manage the CSP plant.

To estimate or predict the solar radiation clear sky atmospheric transmittance is required. The atmosphere is composed of two aerosol particles categories disposed in two dominant layers. The first layer, located at 0-3 km of the Earth's surface, is affected by natural phenomena and anthropogenic activities. The second, called stratospheric dust layer, is located at 15-25 km results from volcanic activities and cosmic rays [2]. Linke proposed a first expression of the atmospheric turbidity: the Linke turbidity coefficient T_L [8]. It represents the number of clean dry atmosphere necessary to produce the observed attenuation of the solar radiation. For example, in Europe, during summer, the water vapor is often large and the blue sky is close to white: T_L is larger than 3. In turbid atmosphere (polluted cities), the T_L is close to 6 - 7. This coefficient was widely used since 1922, because it is easy to implement. However, it is dependant to the airmass [16, 9, 17]. That is why, in 2002, Ineichen and Perez proposed a new formulation of the Linke turbidity coefficient in order to avoid its dependence upon solar geometry and they developed a simple clear sky model for direct normal irradiance [10]. Introducing the Linke turbidity coefficient (T_{LK}) at air mass 2, and a multiplicative coefficient b taking into account the altitude of the site A_S, they obtained the empirical expression of the normal clear sky radiation I_{bn}:

$$I_{bn} = b.I_0.\exp\left(-0.09.AM.\left(T_{LK} - 1\right)\right) \tag{1}$$

$$\text{Where:} \quad b = 0.664 + 0.163/\exp(A_S/8000) \tag{2}$$

I_0 represents the normal incidence extraterrestrial irradiance and AM the altitude corrected air mass [17]. To extract the turbidity factor they inverted the expression (1) and obtained the T_{LIP} value as:

$$T_{LIP} = 1 + \left(11.1 \log\left(\frac{bI_0}{I_{bn}} \right) / AM \right) \quad (3)$$

Consequently, one can easily obtain T_{LIP} knowing the value of the normal clear sky radiation I_{bn} and the geographical parameters of the site (latitude, longitude and altitude). In this present study, the values of the atmospheric turbidity used to develop and validate the predictive models, have been computed using the T_{LIP} expression (3).

Works for hourly meteorological data forecasting (like temperature) have already been mainly developed in the context of short-term or long-term load forecasting and power utilities management . The complex and nonlinear nature of meteorological parameters variations and the abundance of historical data suggest that computational intelligence data-based modeling techniques would be good candidates. In 2011, Marquez and Coimbra developed a solar forecasting model using an Artificial Neural Network (ANN) [21]. For its development and validation, they used predicted meteorological variables from the US National Weather Service's (NWS) forecasting database as inputs. Another work based on artificial intelligence has been presented about solar radiation attenuation in the atmosphere [23]. They developed two models for evaluating atmospheric transmittance using fuzzy logic algorithms. They conclude that fuzzy models are able to perform at least as well as classical models.

The proposed forecast method consists of an adaptive network-based fuzzy inference system based on data selected from the NREL laboratory. A discrete wavelet transform has been applied on this database in order to only select data by clear sky. The ANFIS model is composed of different blocs which give future values of the atmospheric turbidity at several time horizons until 3 hours in order to predict the solar radiation. This paper also presents a study on the influence of model inputs. Indeed, two input sets have been considered: the first one corresponds to the direct meteorological parameters measured while the second derived from a principal component analysis (PCA) on the initial input set.

First, the paper focuses (section 2) on the database selected for the study and on a wavelet-based multi-resolution analysis allowing the model inputs and outputs to be chosen (Fig. 1.a). Section 3 deals with a principal component analysis based on the data in order to find correlations between meteorological variables and to avoid redundant information during the model development (Fig. 1.b). Section 4 describes the neuro-fuzzy methodology used and the proposed side-by-side ANFIS developed (Fig. 1.c). The final part of the paper concludes the present work.

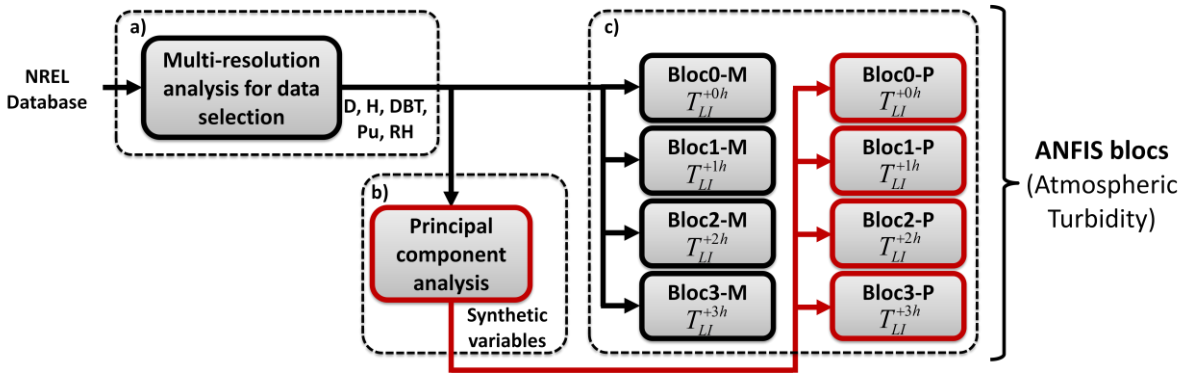

Fig. 1. Diagram of the presented study

2. Database and preliminary analysis

2.1. NREL database

The original database used to develop the atmospheric turbidity model has been collected from the NREL station in Golden, Colorado, USA (Latitude 39.74° N, Longitude 105.18° W, Elevation 1829 m) at http://midcdmz.nrel.gov/apps. Many meteorological parameters are measured as direct normal irradiance, dry bulb temperature, wind speed, wind direction, relative humidity, and pressure. For this study, measurements from 2002 to 2013 with hourly and 1-minute acquisition frequencies have been selected to develop and validate the predictive model. Moreover, since data including the atmospheric turbidity values were necessary, only data by clear sky have been retained. The problematic is to determine when the sky can be considered as clear and thus selecting appropriate data. The method employed is described in the next section.

2.2. Data selection using discrete wavelet multi-resolution analysis

To detect the cloud presence, a wavelet-based multi-resolution analysis was performed using the discrete wavelet transform (DWT). Basically, the discrete wavelet multi-resolution analysis, commonly based on Daubechies orthogonal wavelet basis [6], allows decomposing a signal into approximations and details using respectively low-pass (LP) and high-pass (HP) filters [20]. This process can be repeated *n* times, producing *n* levels of decomposition, but decomposing (downsampling) the approximations (the low frequency coefficients) only (Fig. 3). Indeed, the high frequency coefficients are neglected. So, a signal *x* can be first decomposed into an approximation A_1 and a detail D_1 (that is the level 1 of the decomposition). Then A_1 can be decomposed into an approximation A_2 and a detail D_2 (that is the level 2 of the decomposition) and so on. Considering *n* levels of decomposition, the reconstruction process allows recovering the initial signal *x*, summing the *n* details D_1, D_2, …, D_n and the approximation A_n of level *n*.

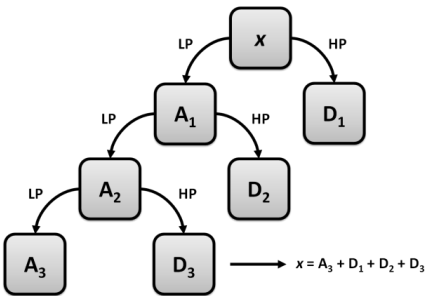

Fig. 2. Multi-resolution analysis leading to the 3-level decomposition of a signal *x*

2.3. Approach

The approach retained to only select clear sky measurements from the NREL database is, in part, based on the details sum D of level *n*. From this value, one can obtain the high frequency of the initial signal. Therefore, a high value, representing a high variation of DNI, can correspond to a passing cloud or a sky partially covered. On the contrary, a low value of D can correspond to a clear sky. However, the value of D can also be low at night or during a very cloudy day, that is why the selection data has been done considering both the signal D and the DNI. From then on, the detection algorithm has been established taking into account a maximum value for D at 3 W and a minimum value for the DNI at 20 $W.m^{-2}$ as the following way:

- *If D<3 AND DNI>20 THEN Decision = 1*
- *ELSE Decision = 0*

where 0 represents a sample not selected and 1 a sample selected. To improve the methodology, two qualitative criteria based on observation have been analyzed from data including passing clouds. These two criteria are: the ability of the system (**k**) to keep good samples (clear sky) and to avoid (**a**) the wrong samples (covered sky). Table 2 highlights the best configuration retained for the data selection. It takes into account a 3-level decomposition (n=3) of the DNI measurement and uses Daubechies wavelets of order 4 (N=4).

Table 1. Parametric study for the wavelet decomposition design

Level decomposition n		Order N of Daubechies wavelets				
		1	2	3	4	5
1	**k**	-	+	+	+	+
	a	+	+	+	+	+
2	**k**	+	-	-	+	+
	a	-	+	+	+	++
3	**k**	+	-	+	++	++
	a	-	+	+	++	++
4	**k**	+	+	+	++	++
	a	-	+	+	++	++

-- inadequate - incomplete + satisfying ++ complete

One can notice in Fig. 3 that data selected with this algorithm for 1 day (07/25/2012) correspond to clear sky instants. Indeed, the variations observed on the DNI measurement curve are not retained by the algorithm to constitute the data selection.

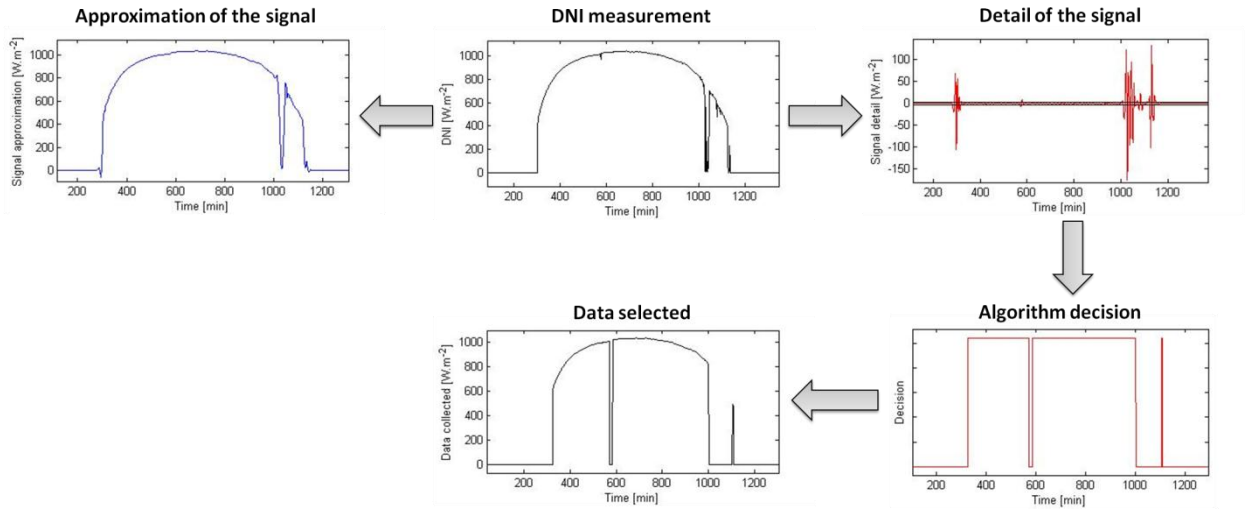

Fig. 3. Decision obtained by discrete wavelet multi-resolution analysis

From this algorithm, the first step of the presented work, it was possible to compute the atmospheric turbidity value at any time by using (3) and then to constitute a full database to specially develop and validate the predictive model.

3. Principal Component Analysis

3.1. Theory

A Principal Component Analysis (PCA) [24, 22] is often used to reduce the number of variables comprising a dataset, retaining the variability in the data. This mathematical procedure uses an orthogonal transformation to convert a set of observations of possibly correlated variables into a set of values of linearly uncorrelated variables: principal components. The number of principal components does not exceed the number of original variables. Thus, this procedure allows first discovering or to reduce the dimensionality of the data set and second to identify new meaningful underlying variables. The objective of this analysis is to minimize redundancy, measured by covariance, and to maximize the signal, measured by variance.

Considering a centered data matrix X arranged as follow:

$$X = \begin{bmatrix} x_1 & x_2 & \cdots & x_m \end{bmatrix}^T \tag{4}$$

one can compute the covariance matrix C_X. X is a m-by-n matrix where m is the number of measured variables and n the number of samples, and C_X is a square symmetric m-by-m matrix defined by:

$$C_X \equiv \frac{1}{n-1} XX^T \tag{5}$$

The diagonal terms of C_X are the variance of particular measurement types and the off-diagonal terms of C_X are the covariance between measurement types. C_X captures the correlations between all possible pairs of measurements. The correlation values reflect the noise and redundancy in measurements. The goal to solve PCA using eigenvectors of covariance is to find some orthonormal matrix P where $Y = PX$ such that C_Y is diagonalized.

$$C_Y \equiv \frac{1}{n-1} YY^T \tag{6}$$

The rows of P are the principal components of X. Rewriting C_Y in terms of the variable P one can obtain:

$$C_Y = \frac{1}{n-1}(PX)(PX)^T = \frac{1}{n-1} PXX^T P^T = \frac{1}{n-1} PAP^T \tag{7}$$

Where $A=XX^T$. The roadmap is to recognize that a symmetric matrix (A) is diagonalized by an orthogonal matrix of its eigenvectors. For a symmetric matrix A defined as:

$$A = EDE^T \tag{8}$$

Where D is a diagonal matrix and E is a matrix of eigenvectors of A arranged as columns. The matrix A has $r \leq m$ orthonormal eigenvectors where r is the rank of the matrix. The rank of A is less than m when A is degenerate or all data occupy a subspace of dimension $r \leq m$. Maintaining the constraint of orthogonality, this situation can be remedied by selecting $(m - r)$ additional orthonormal vectors to "fill up" the matrix E. These additional vectors do not affect the final solution because the variances associated with these directions are zero.

P is selected to be a matrix where each row p_i is an eigenvector of XX^T ($P \equiv E^T$). Thus, with $A = P^T DP$ and $P^{-1} = P^T$, one can finish evaluating C_Y.

$$C_Y = \frac{1}{n-1} PAP^T = \frac{1}{n-1} P(P^T DP)P^T = \frac{1}{n-1} (PP^T)D(PP^T) = \frac{1}{n-1} D \tag{9}$$

The results of PCA can be summarized in the matrices P and C_Y. The principal components of X are the eigenvectors of XX^T or the rows of P, and the i^{th} diagonal value of C_Y is the variance of X along p_i. Finally, one obtain the synthetic data set computing:

$$Y = C_Y{}^T X \tag{10}$$

3.2. Approach

In this case study, meteorological variables are naturally quite possibly correlated with one another. In this objective, the PCA has been applied on a data matrix containing five parameters undeniably influencing the atmospheric turbidity: day, hour, dry bulb temperature, pressure and relative humidity. The objective of this approach is to establish uncorrelated synthetic variables in order to improve the results of the ANFIS model. Indeed, data redundancy leads sometimes to anomalies in the learning phase of the ANFIS and need to be avoided by design.

3.3. Results

Following the previous methodology about the PCA, the C_Y calculation gives:

$$C_Y = \begin{pmatrix} 0.0008 & 0.9997 & 0.0114 & -0.0199 & -0.0095 \\ 0.9992 & -0.0012 & 0.0396 & -0.0033 & 0.0048 \\ 0.0154 & 0.0234 & -0.4196 & 0.6129 & 0.6689 \\ -0.0201 & -0.0082 & 0.3703 & -0.5568 & 0.7432 \\ -0.0309 & 0.0018 & 0.8277 & 0.5603 & 0.0065 \end{pmatrix} \tag{11}$$

Where each column contains coefficients for one principal component. Moreover, the columns have been arranged in descending order of component variance. Thus, the first principal component explains 60.83%, the first two principal components together account for 98.69% of the total variation and the first three account for 99.68% of the variation as show in Table 2.

Table 2. Variances of the 5 components

Components	1st	2nd	3rd	4th	5th
Variance [%]	60.83	37.86	0.99	0.26	0.06
Total variance [%]	60.83	98.69	99.68	99.94	100

The obtained results from the PCA confirm the hypothesis made on possible correlations between meteorological variables. With the first three principal components together, almost the total variation is taken into account (99.68%). However, using only first three components as input of the model, the number of parameters taken into account was considerably reduced and the results were not satisfactory. Therefore, all the five components have been considered for developing the predictive model. The advantage of this method is to have no redundant information between vectors.

4. Prediction

4.1. Neuro-fuzzy theory (NFS)

In the field of artificial intelligence, neural networks and fuzzy logic can be combined in neuro-fuzzy systems in order to achieve both properties of readability and learning ability. Neuro-fuzzy systems synergizes the two techniques by combining the human-like reasoning style of fuzzy systems (through the use of fuzzy sets and a linguistic model consisting of a set of if-then fuzzy rules) with the learning and connectionist structure of neural networks [5, 1]. Various neuro-fuzzy architectures can be found in the scientific literature [12, 13], one can mention: NEFCLASS (classification), FALCON and GARIC (process control), ANFIS (process control, signal processing, non-linear approximation, identification), etc. Because ANFIS is a widely used and powerful architecture, it has been chosen for estimating the thermal diffusivity of building materials, taking into account expert knowledge.

Fuzzy if-then rules are expressions of the form if A then B, where A and B are labels or fuzzy sets characterized by appropriate membership functions. Due to their concise form and through the use of linguistic labels and membership functions, fuzzy if-then rules are often employed to capture the imprecise and subjective modes of reasoning that play a central role in the human ability to make decisions in an uncertain environment [26], [27]. Another form of fuzzy if-then rule, proposed by Takagi and Sugeno, has fuzzy sets involved only in the premise part, the consequent part being described by a non-fuzzy equation of the input variable [25]. Both types of fuzzy if-then rules have been used extensively for modelling and controlling systems. Due to the qualifiers on the premise parts, each fuzzy if-then rule of a set of rules can be considered as a local description of the studied system under consideration.

Fuzzy inference systems (FIS) are also known as fuzzy-rule-based systems or fuzzy controllers when used as controllers. Basically, a fuzzy inference system is composed of five functional blocs [11]: (1) a collection of fuzzy if-then rules; (2) a database which defines the membership functions of the fuzzy sets used to design the fuzzy rules; (3) a decision-making unit allowing performing the inference operations on the rules; (4) a fuzzification interface which transforms the crisp inputs into degrees of match with linguistic values; (5) a defuzzification interface which transforms the fuzzy results of the inference into a crisp output. The steps of fuzzy reasoning performed by fuzzy inference systems can be described as follows: (1) the fuzzification step during which the input variables are compared with the membership functions on the premise part to obtain the membership values of each linguistic label; (2) the combination of the membership values on the premise part to get the weight of each rule of the rule base; (3) the generation of the qualified consequent (fuzzy or crisp) of each rule depending on the weight; (4) the defuzzification step during which the qualified consequents are aggregated to produce a crisp output [18, 19].

The acronym ANFIS derives from adaptive network-based fuzzy inference system. A network-type structure, similar to that of artificial neural networks, which maps inputs through input membership functions and associated parameters and then through output membership functions and associated parameters to output, can be used to interpret an input/output map. The parameters associated with the membership functions changes through the learning process. The adjustment of these parameters is facilitated by a gradient vector. This gradient vector provides a measure of how well the fuzzy inference system is modelling the input/output data for a given set of parameters. When the gradient vector is obtained, any of several optimization routines can be applied in order to adjust the parameters to reduce some error measure [14].

ANFIS architecture: for simplicity, we assume, first, that the considered fuzzy inference system has two inputs x and y and one output z and, secondly, that the rule base contains only two fuzzy if-then rules of Takagi and Sugeno's type [25]. The rules are designed in the following way:

- First rule: *If x is A_1 AND y is B_1 THEN $f_1 = p_1x + q_1y + r_1$*
- Second rule: *If x is A_2 AND y is B_2 THEN $f_2 = p_2x + q_2y + r_2$*

Implementing both rules requires the 5-layer ANFIS architecture shown in Fig. 4 [15]. A membership function $A_i(x)$ or $B_i(y)$, specifying the degree of which x satisfies A_i or y satisfies B_i, with i = 1, 2, is associated with every node in the first layer. Usually $A_i(x)$ and $B_i(y)$ are chosen to be bell-shaped with a minimum and a maximum equal to 0 and 1 respectively:

$$\mu_{A_i}(x) = \frac{1}{1+\left[(x-c_i)/a_i\right]^2 b_i} \quad \text{or} \quad \mu_{A_i}(x) = \exp\left[-\left(\frac{x-c_i}{a_i}\right)^2\right] \tag{12}$$

$$\mu_{B_i}(y) = \frac{1}{1+\left[(y-c_i')/a_i'\right]^2 b_i'} \quad \text{or} \quad \mu_{B_i}(x) = \exp\left[-\left(\frac{y-c_i'}{a_i'}\right)^2\right] \tag{13}$$

with $\{a_i, b_i, c_i\}$and $\{a_i', b_i', c_i'\}$ two parameter sets. As the values of these parameters change, the bell-shaped functions vary accordingly, thus exhibiting various forms of membership functions on linguistic label A_i any continuous and piecewise differentiable functions, such as commonly used trapezoidal or triangular-shaped membership functions, can be used. Nodes in the second layer evaluate the premises of the rules, multiplying the incoming signals and sending the product out. So, the i^{th} node output represents the firing strength of rule i. Let us note that many other T-norm operators, allowing performing generalized AND, can be used in this layer [7]:

$$\omega_i = \mu_{A_i}(x) \times \mu_{B_i}(x) \qquad \text{with i = 1, 2} \tag{14}$$

The i^{th} node in the third layer calculates the ratio of the i^{th} rule's firing strength to the sum of all rules' firing strengths (i.e. the contribution of the i^{th} rule), such as:

$$\overline{\omega}_i = \frac{\omega_i}{\omega_1 + \omega_2} \qquad \text{with i = 1, 2} \tag{15}$$

Nodes in the fourth layer evaluate the conclusions of the rules. So, the i^{th} node evaluates the conclusion of the i^{th} rule, with $\overline{\omega}_i$ the output of layer 3 and $\{p_i, q_i, r_i\}$ a parameter set. Parameters in this layer can be referred as consequent or conclusion parameters. So:

$$\overline{\omega}_i f_i = \overline{\omega}_i (p_i x + q_i y + r_i) \qquad \text{with i = 1, 2} \tag{16}$$

Finally, the single node in the fifth and last layer computes the overall output as the summation of all incoming signals. It is observed that given the values of premise parameters, the overall output can be expressed as a linear combination of the consequent parameters:

$$f = \sum_i \overline{\omega}_i f_i = \frac{\sum_i \omega_i f_i}{\sum_i \omega_i} \qquad \text{with i = 1, 2} \tag{17}$$

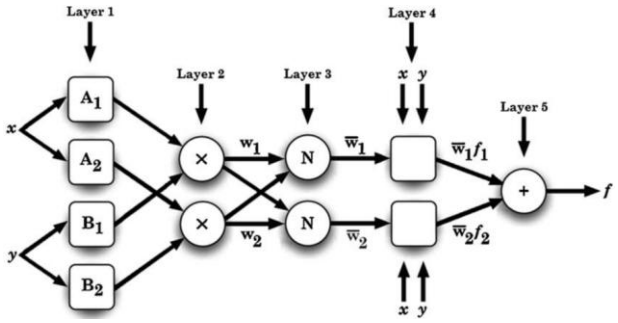

Fig. 4. 5-Layer adaptive network-based fuzzy inference system for the implementation of the two following fuzzy rules: If x is A_1 AND y is B_1 THEN $f_1 = p_1x + q_1y + r_1$ and If x is A_2 AND y is B_2 THEN $f_2 = p_2x + q_2y + r_2$.

To train the ANFIS, a data set that contains the desired input/output data of the system to be modelled is used. The modelling approach is similar to many system identification techniques: first, you hypothesize a parameterized model structure and next, thanks to an iterative and hybrid optimization method, basically a combination of least squares estimation and backpropagation gradient descent method [4], the membership function parameters are adjusted, the consequent parameters are identified and a rule base is designed, according to a chosen error criterion. The training process stops whenever the maximum iteration number is reached or the training error goal is achieved. In general, this type of modelling works well if the training data presented to the ANFIS is fully representative of the features of the data the trained system is intended to model. Checking and testing data sets allow checking the generalization capability of the resulting fuzzy inference system and avoiding overfitting [3].

4.2. Approach

T

4.3. Model development and results

The learning phase involves 55680 examples while 27840 have been selected to the model validation (respectively: 2/3, 1/3) and 84 other days (representing 40320 examples), have been selected for testing the effectiveness of the models (Fig. 5).

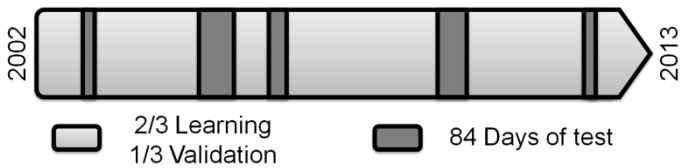

Fig. 5. Learning, validation and test periods used in the database.

Moreover, because we selected a large amount of measurements from the database, all the necessary representative features have been probably collected. Several types of models have been developed and compared. The first one is a model using the five inputs, and the second has been established according to the principal component analysis. In each type of model, several prediction blocs (bloc0, bloc1, bloc2 and bloc3) based on several prediction horizons (at t + 0h, t + 1h, t + 2h and t + 3h) were developed. The Fig. 6 shows the structure of the predictive model using the synthetic variables $V_i(t)$ computed with the PCA.

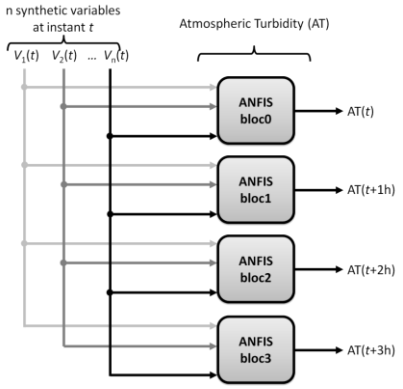

Fig. 6. Structure of the predictive ANFIS model.

From then on, the outputs values of these blocs can be weighted according to the exact prediction horizon desired. To develop each bloc of the model, we focused on the membership functions influence on the results: number and shape. To compare results from different models, we proceeded to an analysis based on the three following criteria: EAM, ERM and FIT, where FIT is defined as:

$$FIT = 1 - \left\| V_{sim} - V_{\exp} \right\|_2 / \left\| V_{\exp} - \left\langle V_{\exp} \right\rangle \right\|_2 \tag{18}$$

We noticed that three membership functions were the better compromise between the number of model parameters to be identified and computation time. For the shape, we tested "Symmetric Gaussian" (SG) and "asymmetric Gaussian" (AG) for their suitability in the field of solar. The obtained results for the atmospheric turbidity forecasting are very close as shown in Table 3. However, the SG membership function type depends on two parameters and the SG membership function type uses one more parameter. Thus the model SG was chosen to estimate the values of the atmospheric turbidity.

Table 3. Membership functions influence on the forecasted and calculated atmospheric turbidity

MAE: mean absolute error; MRE: mean relative error; FIT: similarity criterion.

Atmospheric turbidity	MAE [-]	MRE [%]	FIT [%]
AG	0.07684	2.80	73.09
	0.07725	2.81	73.02
SG	0.07882	2.87	72.04
	0.07912	2.88	71.99

From the three fuzzy sets of Gaussian type, the different blocs (time horizon desired) and the number of examples selected and described previously, the two types of predictive models gave satisfactory results. Table 4 presents the forecasted turbidity at 3 hours (T_{LI}^{+3h}).

From the three fuzzy sets of Gaussian type, the different blocs (time horizon desired) and the number of examples selected and described previously, the two types of predictive models gave satisfactory results (Table 4).

Table 4. Comparison of both the forecasted and calculated atmospheric turbidity at different time-horizons

MAE: mean absolute error; MRE: mean relative error; FIT: similarity criterion.

L: learning phase, V: validation phase, T: test phase

Atmospheric turbidity	Inputs	MAE [-]	MRE [%]	FIT [%]

Instantaneous	Real measurements	L	0.0768	2.80	73.1
		V	0.0773	2.81	73.0
		T	**0.0812**	**2.93**	**71.2**
	From PCA	L	0.0775	2.81	72.5
		V	0.0778	2.82	72.4
		T	**0.0661**	**2.56**	**65.9**
Forecasted at 1 hour (T_{LI}^{+1h})	Real measurements	L	0.0852	3.12	70.7
		V	0.0854	3.12	70.6
		T	**0.0842**	**2.98**	**69.4**
	From PCA	L	0.0805	2.91	71.2
		V	0.0808	2.92	71.1
		T	**0.0678**	**2.62**	**65.5**
Forecasted at 2 hours (T_{LI}^{+2h})	Real measurements	L	0.0871	3.18	69.7
		V	0.0874	3.19	69.6
		T	**0.0863**	**3.12**	**68.1**
	From PCA	L	0.0885	3.22	68.7
		V	0.0890	3.24	68.5
		T	**0.0898**	**3.26**	**67.7**
Forecasted at 3 hours (T_{LI}^{+3h})	Real measurements	L	0.0875	3.19	68.3
		V	0.0878	3.20	68.15
		T	**0.0943**	**3.29**	**67.3**
	ACP	L	0.0813	2.97	71.6
		V	0.0816	2.98	71.5
		T	**0.0825**	**3.05**	**70.9**

However, in each model, the errors between the predicted and experimental values naturally increase when the prediction horizon is higher.

Moreover, between the two types of models developed, one can note slightly better results from the model using inputs established by the PCA. For example, with the model using the meteorological variables as inputs in bloc3, the MAE, the MRE and the FIT are respectively 0.0875, 3.19% and 68.3% and with the model using the inputs established by the PCA, the same criteria are about 0.0825, 3.05% and 70.89%.

Between the two types of models developed, one can note slightly better results from the model using inputs established by the PCA. In the bloc3 using the meteorological variables as inputs, the MAE, the MRE and the FIT are respectively 0.094, 3.29% and 67.28% and with the model using the inputs established by the PCA, the same criteria are about 0.083, 3.05% and 70.89%.

4. Conclusion

As part of the CSPIMP project, the present paper focuses on forecasting the atmospheric turbidity with the aim of optimizing the solar resource prediction. To develop, validate and test our predictive models of the atmospheric turbidity, measurements from the NREL laboratory were selected from 2002 to 2013 with hourly and 1-minute acquisition frequencies. From this database, only data corresponding to clear sky days have been considered by using wavelet-based multi-resolution analysis. Moreover, after a principal component analysis on meteorological variables, we identified new five meaningful underlying variables avoiding redundant information. Then, we compared two different types of model, both based on a side-by-side ANFIS and including four blocs for prediction

at different time horizons (T_{LI}^{+0h}, T_{LI}^{+1h}, T_{LI}^{+2h}, and T_{LI}^{+3h}). As a result of the study about the atmospheric turbidity forecasting, the chosen configuration, leading to accurate forecasts (the MAE, the MRE and the FIT are respectively about 0.083, 3.05% and 70.89%), is defined with: 4 blocs (4 time horizons), 3 membership functions (SG type) and 5 inputs (day, hour, outdoor temperature, pressure and relative humidity or five synthetic variables issues to the PCA). These results validate the proposed methodology and highlight both the impact of working with principal component analysis and the learning capability of adaptive network-based fuzzy inference system.

References

[1] A. Abraham. Adaptation of fuzzy inference system using neural learning. *fuzzy system engineering: theory and practice, in: N. Nedjah, et al. (Eds.), Studies in Fuzziness and Soft Computing, Springer Verlag, Germany.*, vol. 3:pp. 53–83., 2005.

[2] WE Alnaser and NS Awadalla. The linke turbidity factor and ångström coefficient in humid climate of bahrain. *Earth, Moon, and Planets*, 70(1-3):61–74, 1995.

[3] W. Brauer C. Schittenkopf, G. Deco. Two strategies to avoid overfitting in feedforward networks. *Neural Networks*, 10:505–516, 1997.

[4] C. Charalambous. Conjugate gradient algorithm for efficient training of artificial neural networks. *IEEE Proceedings*, 139:301–310, 1992.

[5] C.S.G. Lee C.T. Lin. Neural fuzzy systems: A neuro-fuzzy synergism to intelligent systems. *Prentice Hall, Upper Saddle River, NJ*, 1996.

[6] Ingrid Daubechies et al. *Ten lectures on wavelets*, volume 61. SIAM, 1992.

[7] E. Pap E.P. Klement, R. Mesiar. Triangular norms. *Kluwer Academics Publishers, Dordrecht, The Netherlands*, 2000.

[8] Linke F. Transmisions-koeffizient und trübungsfaktor. *Beitr. Physik. fr. Atmos.*, 10:91–103, 1922.

[9] JC Grenier, A de La Casinière, and T Cabot. A spectral model of linke's turbidity factor and its experimental implications. *Solar Energy*, 52(4):303–313, 1994.

[10] Pierre Ineichen and Richard Perez. A new airmass independent formulation for the linke turbidity coefficient. *Solar Energy*, 73(3):151 – 157, 2002.

[11] J.S.R. Jang. Anfis: adaptative-network-based fuzzy inference system. *IEEE Transactions on Systems, Man, and Cybernetics*, 23 (3):665–685, 1993.

[12] Y. Hayashi J.J. Buckley. Fuzzy neural networks: a survey. *Fuzzy Sets and Systems*, 66:1–13, 1994.

[13] Y. Hayashi J.J. Buckley. Neural networks for fuzzy systems. *Fuzzy Sets and Systems*, 7:265–276., 1995.

[14] C.T. Sun J.S.R. Jang. Neuro-fuzzy modeling and control. *IEEE Proceedings*, 83 (3):378–406, 1995.

[15] H. White K. Hornik, M. Stinchcombe. Multi-layer feedforward networks are universal approximation. *Neural Networks*, 2:359–366, 1989.

[16] F Kasten. Elimination of the virtual diurnal variation of the linke turbidity factor. *Meteorologische Rundschau*, 41(3):93–94, 1988.

[17] Fritz Kasten and Andrew T Young. Revised optical air mass tables and approximation formula. *Appl. Opt*, 28(22):4735–4738, 1989.

[18] C.C. Lee. Fuzzy logic in control systems: fuzzy logic controller - part i. *IEEE Transactions on Systems, Man, and Cybernetics*, 20:404–418, 1990.

[19] C.C. Lee. Fuzzy logic in control systems: fuzzy logic controller - part ii. *IEEE Transactions on Systems, Man, and Cybernetics*, 20:419–435, 1990.

[20] Stéphane Mallat. *A wavelet tour of signal processing*. Access Online via Elsevier, 1999.

[21] Ricardo Marquez and Carlos F.M. Coimbra. Forecasting of global and direct solar irradiance using stochastic learning methods, ground experiments and the {NWS} database. *Solar Energy*, 85(5):746 – 756, 2011.

[22] Achmad Muslim, Toni Bakhtiar, et al. Variable selection using principal component and procrustes analyses and its application in educational data. *Journal of Asian Scientific Research*, 2(12):856–865, 2012.

[23] Marius Paulescu, Paul Gravila, and Eugenia Tulcan-Paulescu. Fuzzy logic algorithms for atmospheric transmittances of use in solar energy estimation. *Energy Conversion and Management*, 49(12):3691 – 3697, 2008.

[24] Jonathon Shlens. A tutorial on principal component analysis. *Systems Neurobiology Laboratory, University of California at San Diego*, 2005.

[25] M. Sugeno T. Takagi. Derivation of fuzzy control rules from human operator's control actions. *in: Proc. IFAC Symp. Fuzzy Inform., Knowledge Representation and Decision Analysis*, page 55–60, 1983.

[26] L. Zadeh. Fuzzy sets. *Information and Control*, 8:338–353, 1965.

[27] L. Zadeh. Outline of a new approach to the analysis of complex systems and decision processes. *IEEE Transactions on Systems, Man, and Cybernetics*, 3:28–44, 1973.